The E1 Copper Binding Domain of Full-Length Amyloid Precursor Protein Promotes Epithelial to Mesenchymal Transition in DU145 Cells in an Isoform-Specific Manner

Mallory Gough[1], Craig Delury[1] and Edward Parkin[1*]

[1]*Division of Biomedical and Life Sciences, Faculty of Health and Medicine, Lancaster University, Lancaster, LA1 4YQ, U.K.*

Authors' contributions

Author EP designed the study, performed the statistical analysis, wrote the protocol, and wrote the first draft of the manuscript. All authors managed the analyses of the study and read and approved the final manuscript.

Original Research Article

ABSTRACT

Epithelial to mesenchymal transition (EMT) confers migratory and dynamic properties on cells and, as such, plays a pivotal role in the development of metastatic, castration resistant prostate cancer. The amyloid precursor protein (APP), although most closely associated with the neurodegenerative condition Alzheimer's disease, has also been linked to the pathogenesis and prognosis of several cancers including prostate cancer.
Aims: To investigate whether over-expression of APP could promote EMT in prostate cancer (PCa) DU145 cells and to determine the molecular prerequisites for this effect.
Methodology: A range of APP molecular constructs were stably expressed in DU145 cells and their effects on EMT were monitored by morphological analysis and by immunoblotting for the EMT

Corresponding author: E-mail: e.parkin@lancaster.ac.uk;

marker proteins, E-cadherin and vimentin.

Results: Our results show that the full-length 695 amino acid isoform (APP$_{695}$), but not APP$_{751}$ or APP$_{770}$, promoted EMT via a mechanism requiring an intact extracellular E1 copper binding domain and tyrosine687 within the cytosolic domain of the protein.

Conclusion: Targeting the expression of APP$_{695}$ or the E1 copper binding domain of the protein may, therefore, contribute to therapeutic strategies for the delay or prevention of prostate cancer metastasis.

ABBREVIATIONS

Aβ, amyloid beta; AD, Alzheimer's disease; APP, amyloid precursor protein; BACE1, beta-site APP-cleaving enzyme 1; CuBD, copper binding domain; EMT, epithelial to mesenchymal transition; ICD, intracellular domain; PCa, prostate cancer; RT-PCR, reverse transcription polymerase chain reaction; sAPPα, soluble APP alpha; sAPPβ, soluble APPbeta; SDS-PAGE, sodium dodecyl sulphate-polyacrylamide gel electrophoresis

1. INTRODUCTION

Advanced, androgen-independent, chemo-refractory prostate cancer (PCa) remains incurable. Thus, the identification of new therapeutic targets for the treatment/prevention of metastatic disease would reduce disease mortality.

Epithelial to mesenchymal transition (EMT) is the process by which a polarized epithelial cell assumes a mesenchymal phenotype and facilitates the malignant transformation and metastasis of prostate cancer cells [1-3]. The process begins with a decrease in cellular E-cadherin levels leading to the mechanical disruption of adherens junctions and reduced cell-cell and cell-matrix interactions [4]. E-cadherin is replaced by N-cadherin whilst other proteins such as vimentin and fibronectin replace cytokeratin expression [4]. The repression of proteins that promote EMT might represent a viable therapeutic strategy for the prevention of PCa metastasis.

The amyloid precursor protein (APP) has achieved notoriety for its role in the pathogenesis of the neurodegenerative condition, Alzheimer's disease (AD). Three major isoforms of the protein are expressed in human tissues, APP$_{695}$, APP$_{751}$ and APP$_{770}$ [5]. The main components of the extracellular senile plaques in the AD-afflicted brain are amyloid beta (Aβ)-peptides which are derived from APP through two sequential proteolytic cleavages by β-secretase (β-site APP-cleaving enzyme 1; BACE1) and the γ-secretase complex [5]. The initial soluble product generated by β-secretase is termed sAPPβ (soluble APP beta). In contrast to this 'amyloidogenic' pathway, APP is also processed via a non-amyloidogenic route involving α-secretase cleavage within the Aβ domain [5]. This latter cleavage precludes Aβ-peptide formation and generates sAPPα (soluble APP alpha).

More recently, APP has been shown to play a role in cancer. Expression of the protein stimulates colon carcinoma cell proliferation [6] and an increase in APP mRNA expression in oral squamous cell carcinomas is associated with a reduction in patient survival [7]. Thyroid cancers are characterized by up regulation of APP protein and mRNA expression [8] with the former also being enhanced in pancreatic tissue specimens [9]. Of particular relevance in the current context, Takayama et al. [10] demonstrated that *APP* is an androgen-regulated gene and that expression levels of the protein in PCa LNCaP cells positively correlated with cell proliferation. Higher APP protein expression level in PCa tissue specimens also correlated with a poorer disease prognosis. More recently, Miyazaki et al. [11] published data demonstrating that the proliferation and invasion of two PCa cell lines (LNCaP and DU145) were impaired following the depletion of the endogenous protein. The authors also demonstrated a down-regulation in EMT-related genes in these cell lines following APP-depletion.

In the current study, we have examined whether the over-expression of APP isoforms can promote EMT in DU145 cells and investigated the molecular prerequisites for such an effect. Our results show that APP$_{695}$ enhances EMT

changes in an isoform-specific manner via a mechanism requiring intact E1 copper binding and cytosolic domains of the protein.

2. MATERIALS AND METHODS

2.1 Materials

Anti-APP C-terminal and anti-actin monoclonal antibodies were from Sigma-Aldrich (Poole, U.K.). Anti-APP 6E10 monoclonal antibody was from Cambridge Bioscience Ltd. (Cambridge, U.K.) and anti-sAPPβ (1A9) antibody was kindly provided by Ishrut Hussain (GlaxoSmithKline, Harlow, U.K.). Monoclonal antibody 22C11 was from Millipore (Watford, U.K.). Anti-E-cadherin and anti-vimentin polyclonal antibodies were from R&D Systems (Minneapolis, U.S.A.). APP mutant DNA constructs were either synthesized in-house by site-directed mutagenesis of a wild-type APP_{695} template or *de novo* by Epoch Life Science Inc. (Missouri City, U.S.A.). All other materials, unless otherwise stated, were from Sigma-Aldrich (Poole, U.K.).

2.2 Cell Culture

All cell culture reagents were purchased from Lonza Ltd. (Basel, Switzerland). DU145 cells were cultured in Roswell Park Memorial Institute (RPMI) 1640 medium supplemented with 25 mM glucose, 4 mM L-glutamine, 10% (v/v) foetal bovine serum, penicillin (50 U/ml), streptomycin (50 mg ml^{-1}), and fungizone (2.5 mg ml^{-1}). Cells were maintained at 37^{0}C in 5% CO_2 in air. Stable DU145 transfectants were generated using the Amaxa cell line Nucleofector Kit L in a Nucleofector 2b device (Lonza Ltd., Basel, Switzerland) and subsequent selection of stable transfectants was performed using hygromycin B (200 μg ml^{-1}). For the experiments involving the truncated sAPPα and sAPPβ constructs, plasmids were stably expressed in SH-SY5Y (sAPPα) or HEK (sAPPβ) cells. Medium conditioned for 48 h on mock-, sAPPα- and sAPPβ-transfected cells was then harvested, centrifuged at 100, 000 *g* for 1 h, and concentrated 50-fold in centrifugal concentrators (Sartorius, Epsom, U.K.) before being reconstituted to the original volume in Opti-MEM (Lonza Ltd., Basel, Switzerland). This reconstituted, pre-conditioned medium was then incubated for 24 h with mock-transfected DU145 cells before replacing with fresh pre-conditioned medium and incubating for a further 24 h.

2.3 Reverse Transcription Polymerase Chain Reaction (RT-PCR)

Total RNA was extracted using an RNA extraction kit according to the manufacturer's instructions (Qiagen, Crawley, U.K.) and RNA concentrations were determined using a Nanodrop 2000c spectrophotometer reading at a wavelength of 260 nm (Thermo Scientific, St Leon-Rot, Germany). Total RNA levels were equalized between samples and RT-PCR reactions for APP isoforms and actin were performed using a Titanium One-step RT-PCR kit (BD Biosciences, Oxford, U.K.) according to the manufacturer's instructions. Primers and RT-PCR reaction conditions have been described previously [12].

2.4 Protein Assay

Protein was quantified using bicinchoninic acid [13] in a microtitre plate with bovine serum albumin (BSA) as a standard.

2.5 Sodium Dodecyl Sulphate Polyacrylamide Gel Electrophoresis (SDS-PAGE) and Immunoelectrophoretic Blot Analysis

Samples were mixed with a half volume of reducing electrophoresis sample buffer and boiled for 3 min. Proteins were resolved by SDS-PAGE using 7-17% polyacrylamide gradient gels and transferred to Immobilon P polyvinylidenedifluoride (PVDF) membranes as previously described [14]. Anti-APP C-terminal antibody detects an epitope within amino acids 676-695 (APP_{695} numbering) of the APP cytosolic domain and, therefore, detects all full-length APP isoforms; it was used at a dilution of 1:7500. Anti-APP 6E10 detects an epitope within amino acid residues 3-8 of the Aβ region of APP and, therefore, detects both full-length and sAPPα forms of all three major APP isoforms; it was used at a dilution of 1:2500. Anti-sAPPβ (1A9) detects a neoepitope formed at the C-terminus of sAPPβ following β-secretase cleavage of full-length APP and, therefore, specifically detects the sAPPβ forms of all three major APP isoforms; it was used at 1:3000. Antibody 22C11 detects an epitope within amino acid residues 66-81 of the N-terminal ectodomain of APP and, therefore, detects all soluble and full-length forms of all three major APP isoforms; it was used at 1:1000. Anti-actin was used at 1:5000 whilst the anti-E-cadherin and anti-vimentin antibodies were both used at 1:2000.

Bound antibody was detected using peroxidase-conjugated secondary antibodies (Sigma-Aldrich, Poole, U.K. and R&D Systems Europe Ltd., Abingdon, U.K.) in conjunction with enhanced chemiluminescence detection reagents (Perbio Science Ltd, Cramlington, U.K.).

2.6 Light Microscopy and Dendricity Analysis

A Nikon (Surrey, U.K.) eclipse TE200 optical microscope was used in conjunction with a Nikon COOLPIX P6000 digital camera to produce cell images. Dendricity factor analysis was performed by calculating the area and perimeter of ten randomly selected cells (using points of a superimposed grid to choose individual cells for analysis) using image J software. These data points were then utilised to calculate dendricity factor using the equation $P^2/4\pi A$ when P = perimeter of cell and A = area of cell.

2.7 Statistical Analysis

All data are presented as the means ± S.D. Data were subjected to statistical analysis via Student's t-test. Levels of significance are indicated in the figure legends.

3. RESULTS AND DISCUSSION

Initially we examined which APP isoforms were endogenously expressed in DU145 cells using semi-quantitative RT-PCR (measurements at the protein level in cell lysates are hindered by the existence of multiple co-migrating glycoforms of each isoform). Note that this experiment was not designed to accurately quantify the individual APP isoforms merely to determine which isoforms were present for subsequent over-expression studies. Therefore, it was not necessary to perform real time quantitative PCR. The results (Fig. 1A) revealed three main RT-PCR products generated from the DNA of mock (vector only)-transfected DU145 cells. These bands, at 562, 505 and 337 base pairs, corresponded to the expected product sizes for APP_{770}, APP_{751} and APP_{695}, respectively. The identity of the smallest band was confirmed as APP_{695} by conducting the same experiment using template DNA isolated from APP_{695}-transfected DU145 cells. Note that slight increases in the larger APP isoform products were also observed in APP_{695}-transfected cells; we believe that this is due to the weak ability of transfected APP_{695} to self-regulate the expression of the endogenous protein as observed previously [15]. Although only semi-quantitative, these data were sufficient

to demonstrate that the main APP isoforms present in DU145 cells are APP_{770} and APP_{751}, with lesser amounts of APP_{695}.

Given the lower endogenous background levels of APP_{695}, we initially examined the effects of over-expressing this isoform on EMT. Following the stable transfection of DU145 cells, full-length over-expressed APP_{695} was detected in cell lysates by immunoblotting as two main bands at around 110 kDa (representing the immature and fully glycosylated mature forms of the protein, respectively) (Fig. 1B). The α-secretase-cleaved forms of APP_{751} and APP_{770} (sAPPα) in conditioned medium co-migrated as a single band whilst transfected APP_{695} was detected as a slightly smaller band migrating below the larger protein isoforms (Fig. 1C). Note that only mature APP reaches the cell surface and is subsequently cleaved by secretase activity such that the detection of the different isoforms in conditioned medium is not confused by the presence of multiple glycoforms. Although roughly equivalent amounts of sAPPα were generated from APP_{695} and the larger protein isoforms, we observed, as others have done so previously [16], that sAPPβ was generated almost exclusively from the smaller isoform (Fig. 1C).

Having confirmed the over-expression of APP_{695}, we next examined the effects of the protein on EMT in DU145 cells. Light microscopy images revealed EMT-like changes in morphology following APP_{695} transfection with cells exhibiting a more independent growth pattern with many more membrane protrusions (Fig. 2A). As would be expected following EMT [4], levels of E-cadherin decreased 60% in APP_{695}-transfected cells whilst vimentin levels increased 4.6-fold (Fig. 2B).

We next examined the APP molecular prerequisites for the promotion of EMT by generating a range of APP constructs (Fig. 3). Immunoblot data documenting the relative expression and generation of proteolytic fragments from these constructs have been reported previously by our group [17] and, therefore, are presented only in summarised table format in the current manuscript (Table 1). Initially we examined whether the larger APP_{751} and APP_{770} isoforms could elicit EMT in a similar manner to their smaller APP_{695} counterpart (Fig. 3A). These holoproteins were over-expressed in DU145 cells to the same level as APP_{695} and the levels of sAPPα generated were

not significantly different (Table 1). In contrast, the levels of sAPPβ generated from the two larger isoforms were significantly less than from APP$_{695}$ (Table 1). Changes in EMT were quantified in terms of the relative dendricity of the different cell lines (see Materials and Methods section). APP$_{695}$ enhanced dendricity by 153% relative to mock-transfected cells (Table 1) whereas the two larger APP isoforms had no significant effect. Thus, the ability to promote EMT was specific to the APP$_{695}$ isoform and, as such, all further constructs investigated were based on this smaller isoform.

As the amount of sAPPβ generated from APP$_{695}$ was greater than from APP$_{751}$ or APP$_{770}$, we postulated that the soluble forms of the protein generated by α- or β-secretase activity might be capable of promoting EMT. Therefore, we generated constructs analogous to these fragments truncated C-terminally to lysine612 (sAPPα) and methionine596 (sAPPβ (Figs. 3B and 3C). Unfortunately, when the former construct was expressed in DU145 cells, the product was aberrantly processed intracellularly (Figs. 4A and 4B). However, when expressed in alternative cell lines (HEK or SH-SY5Y) the two constructs were secreted as the predicted fragments of approximately 110 kDa (Figs. 4C and 4D). We, therefore, incubated mock-transfected DU145 cells with conditioned medium from these alternate cell lines (see Materials and Methods section) but both constructs failed to promote EMT (Table 1). Also of note is the fact that α- and β-secretase inhibitors had no effect on the morphology of APP$_{695}$-transfected DU145 cells (data not shown).
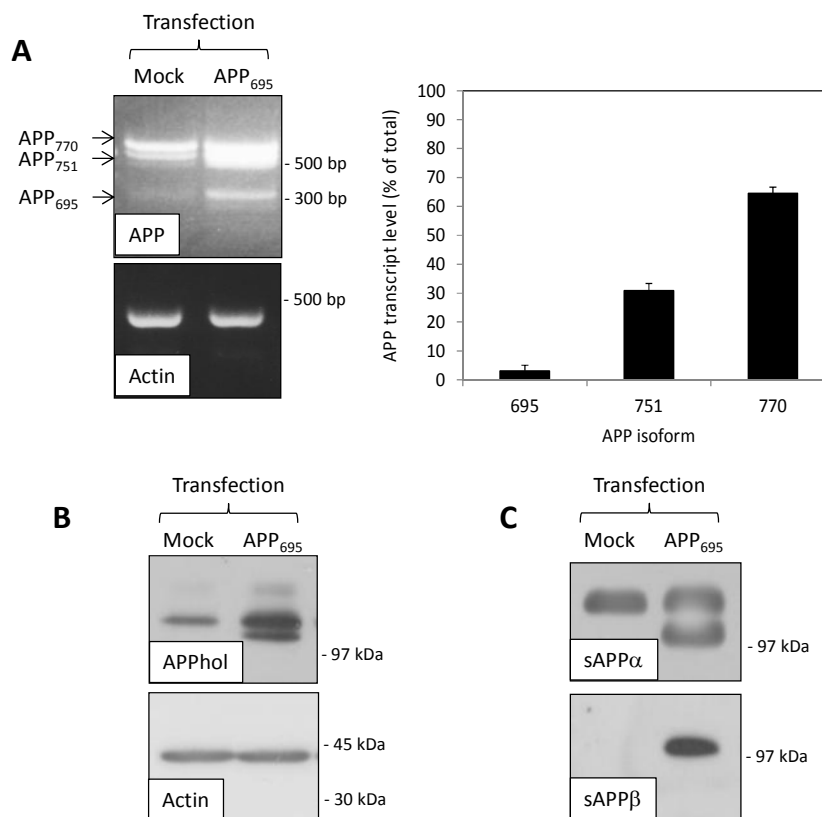

Fig. 1. Expression and proteolysis of APP in DU145 cells
A. Semi-quantitative RT-PCR analysis of APP isoform transcript levels in mock- (vector only) and APP695-transfected DU145 cells. A graphical quantification of the relative levels of endogenous DU145 APP transcripts is shown; results are means ± S.D. (n=3). An actin RT-PCR is also shown in order to confirm equal template DNA concentrations in the reactions. B. Immunoblot analysis of APP holoprotein and actin levels in mock- and APP695-transfected DU145 cell lysates. C. Immunoblot analysis of sAPPα and sAPPβ levels in conditioned medium from mock- and APP695-transfected DU145 cells.

Table 1. Expression and proteolysis of APP constructs and their effects on the relative dendricity of DU145 cells

Construct transfected	Uncleaved protein in cell lysates	sAPPα in conditioned medium	sAPPβ in conditioned medium	Relative dendricity
Mock (empty vector)	N/A	N/A	N/A	100%
APP$_{695}$	100 %	100 %	100 %	**153.0 ± 16.6 %***
APP$_{751}$	98.2 ± 4.6 %	97.6 ± 8.7 %	**36.7 ± 12.1 %***	99.9 ± 5.6 %
APP$_{770}$	102.1 ± 10.2 %	98.3 ± 13.2 %	**53.6 ± 13.9 %***	102.8 ± 3.7 %
sAPPα	N/A	**362.5 ± 38.9 %****	N/A	86.3 ± 14.4 %
sAPPβ	N/A	N/A	**465.3 ± 67.3 %****	98.1 ± 5.9 %
APPΔICD	87.3 ± 19.4%	93.9 ± 21.4 %	**0**	105.4 ± 10.1 %
APP Y682G	97.4 ± 18.3 %	101.8 ± 12.5 %	**36.7 ± 21.2 %***	**161.2 ± 33.1 %***
APP Y687G	101.3 ± 21.6 %	89.2 ± 19.9 %	**56.1 ± 12.3 %****	97.1 ± 8.2 %
APP Y682+687G	89.9 ± 20.5 %	95.0 ± 16.7 %	**24.1 ± 11.3 %****	96.2 ± 7.8 %
APPΔCuE1	112.6 ± 17.3%	97.0 ± 12.9 %	101.2 ± 21.6 %	81.5 ± 18.5%

*The expression and proteolytic fragment formation levels are expressed relative to those detected in APP$_{695}$-transfected cells. The relative dendricity results are expressed relative to mock (vector only)-transfected cells. Results are means ± S.D. (n=3). N/A = not applicable. Statistically significant differences are in bold type. * and ** denote significance at P = .01 and P = .005, respectively.*

The fact that soluble forms of APP failed to promote EMT suggested that the intracellular domain (ICD) of the protein might be a prerequisite in this respect. Therefore, we generated a construct (APPΔICD) truncated C-terminally to residue 648 (Fig. 3D). Following transfection into DU145 cells, the expression level of APPΔICD was identical to that of wild-type APP$_{695}$ as was the level of sAPPα generated from the two proteins (Table 1). However, no sAPPβ was generated from the former construct which was probably indicative of the fact that the APP ICD is required for internalisation of the protein and subsequent β-secretase cleavage. However, given our previous results showing that sAPPβ had no effect on EMT, the fact that the APPDICD construct failed to promote the process (Table 1) was almost certainly due to the lack of intracellular domain rather than a change in sAPPβ generation.

In order to narrow down the involvement of the APP ICD in EMT, we examined the role of two cytosolic tryosine residues within this domain (tyrosines682 and 687) the phosphorylation of which might be linked to cell signalling. Three constructs were generated; APP Y682G, APP Y687G and APP Y682+687G (Fig. 3E) and the corresponding holoproteins were found to

express to similar levels as that of wild-type APP$_{695}$ in DU145 cells (Table 1). Whilst the levels of sAPPα generated from these constructs were not statistically different to that generated from the wild-type protein, the levels of sAPPβ were reduced (Table 1). Interestingly, the single Y682A mutant promoted EMT to a similar extent as wild-type APP$_{695}$ (Table 1), despite a decreased generation of sAPPβ adding further support to the fact that the generation of this fragment was not a prerequisite. However, both the APP Y687A and the APP Y682+687A mutants were unable to promote EMT indicating that the tyrosine residue at position 687 but not at position 682 was required in this respect.

Finally, we examined the role of the copper binding domain (CuBD) in the E1 extracellular domain of APP in relation to EMT. We generated a construct (APPΔCuE1) in which three histidines were mutated to alanine in a key area of the protein associated with copper binding [18] (Fig. 3F). This construct was expressed and processed in DU145 cells in a manner identical to that of wild-type APP$_{695}$ (Table 1). However, APPΔCuE1 failed to promote EMT indicating that the extracellular E1 CuBD, in addition to the cytosolic domain, of APP were prerequisites in this respect.
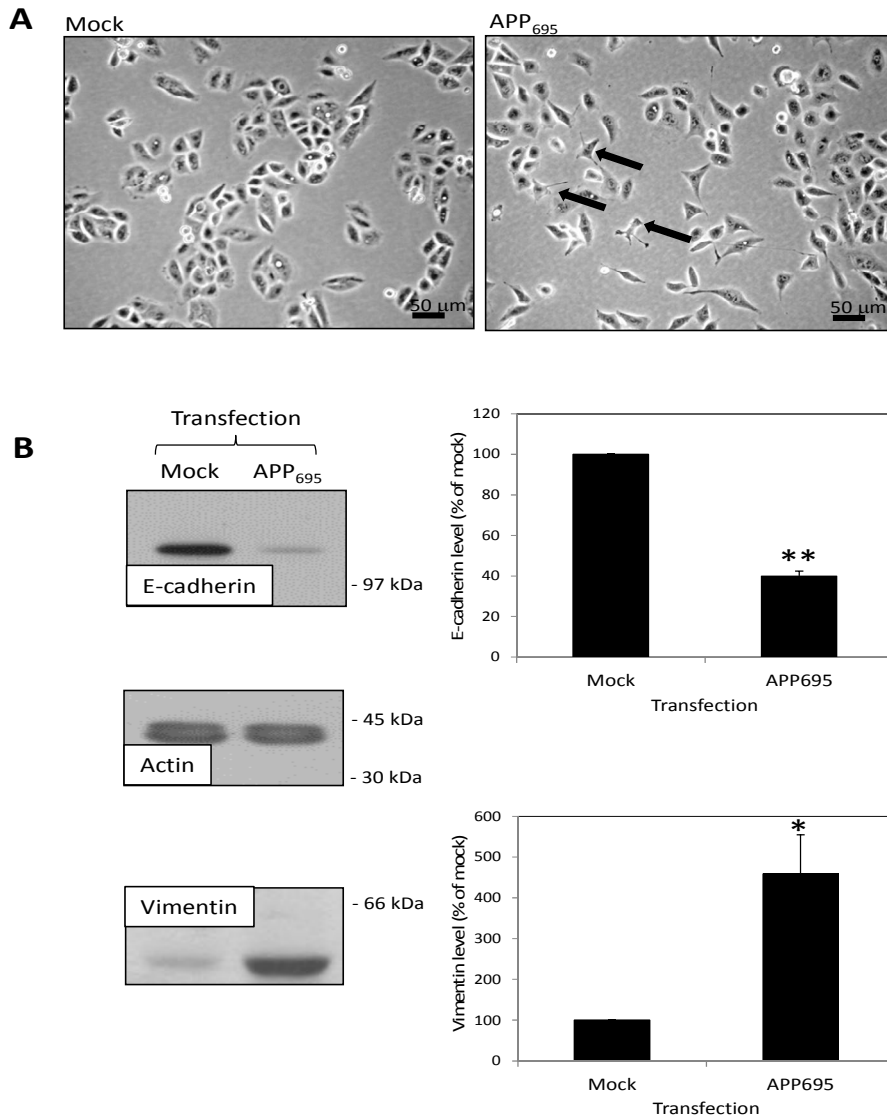
Fig. 2. APP$_{695}$ promotes epithelial to mesenchymal transition in DU145 cells

*A. Microscopy images of mock- and APP$_{695}$-transfected DU145 cells. The arrows on the right hand image are incorporated in order to highlight some of the more dramatic morphological changes observed in the APP$_{695}$-transfected cells. B. Immunoblot analysis of E-cadherin and vimentin levels in mock- and APP$_{695}$-transfected DU145 cell lysates. Graphical quantification of the relative levels of the two proteins are also shown; results are means ± S.D. (n=3). * and ** denote significance at P = .01 and P = .005, respectively. An actin immunoblot is also shown in order to confirm equal total protein levels between samples.*
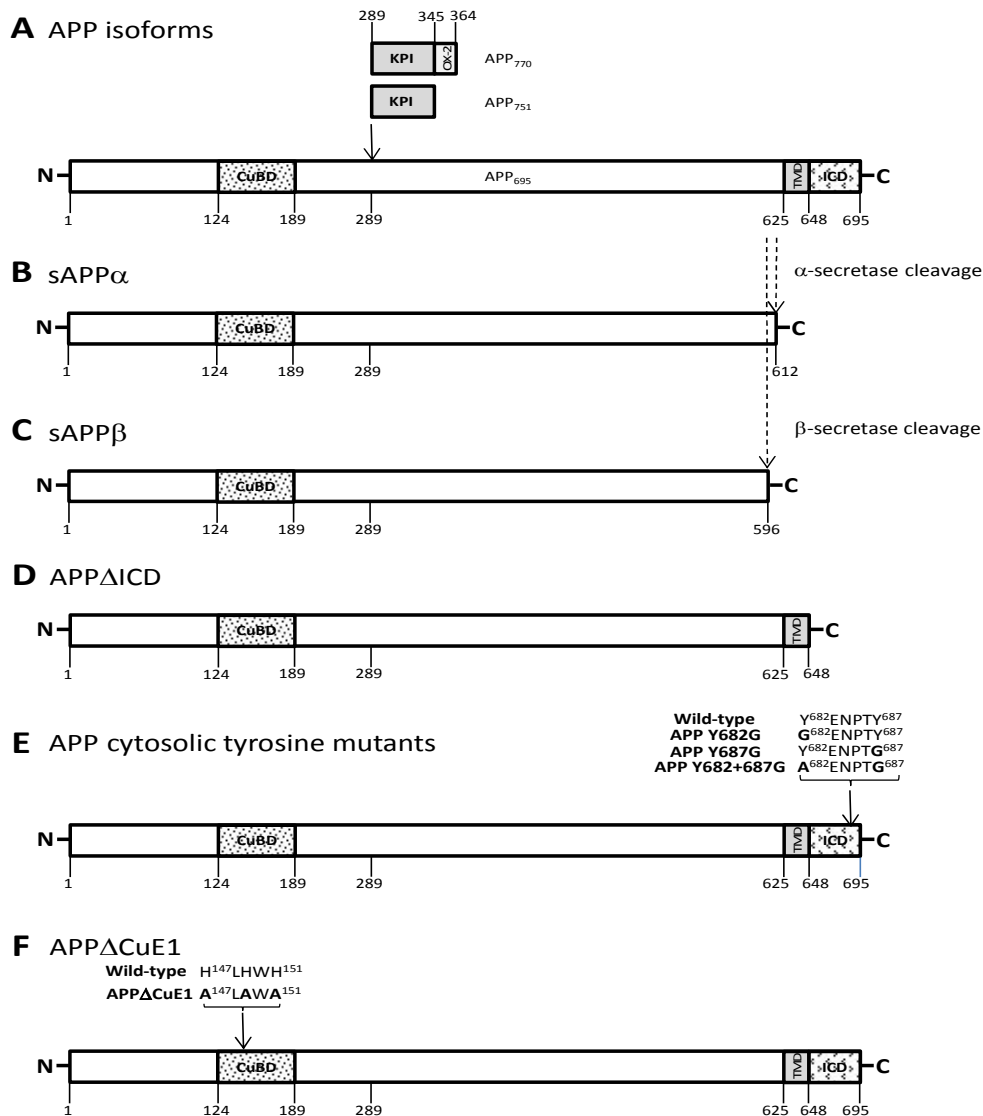
Fig. 3. A schematic detailing the APP constructs employed

A. The APP$_{770}$ isoform possesses both Kunitz protease inhibitor (KPI) and OX-2 domains between residues 289 and 364. APP$_{751}$ lacks the latter domain and APP$_{695}$ lacks both domains. All additional constructs were based on the APP$_{695}$ isoform. B. The sAPPα construct is analogous to soluble APP cleaved from the holoprotein by α-secretase activity and is, therefore, truncated C-terminally to lysine612. C. The sAPPβ construct is analogous to soluble APP cleaved from the holoprotein by β-secretase activity and is, therefore, truncated C-terminally to methionine596. D. The APP∆ICD construct is truncated after the transmembrane domain (TMD) and, therefore, lacks the intracellular domain (ICD) of the wild-type protein. E. The APP cytosolic tyrosine mutants have tyrosine to glycine mutations in the ICD at positions 682 (APP Y682G), 687 (APP Y687G) or at both of these residues (APP Y682G+687G). F. The APP∆CuE1 construct possesses three histidine to alanine mutations at positions 147, 149 and 151 within the E1 copper binding domain (CuBD) of the protein.
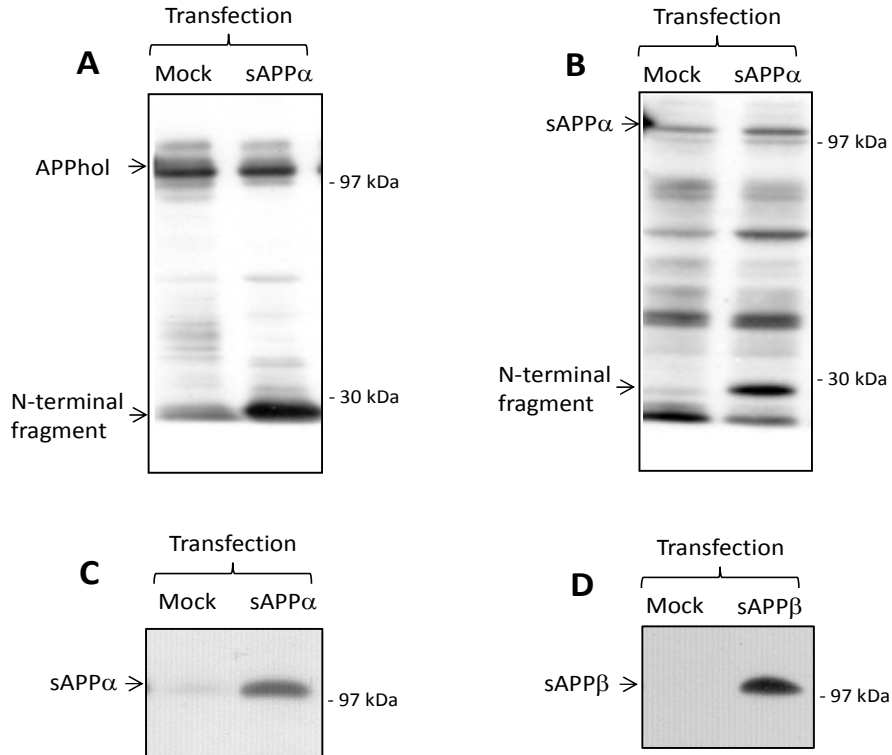
8

Fig. 4. Soluble APP construct expression

*Stable expression of the sAPPα construct in DU145 cell lysates (**A**) and conditioned medium (**B**). APP and its proteolytic fragments were detected using antibody 22C11. The over-expressed construct was detected as an unexpected N-terminal fragment at 25 kDa in both lysates and conditioned medium. Levels of sAPPα at the expected molecular mass of 110 kDa were not changed significantly. **C.** Detection of the sAPPα construct in pre-conditioned medium from stably transfected SH-SY5Y cells using anti-APP antibody 6E10. **D.** Detection of the sAPPβ construct in pre-conditioned medium from stably transfected HEK cells using antibody 1A9. Note that, in the two latter panels, the over-expressed sAPP was detected at the correct predicted molecular mass for the fragments.*

4. CONCLUSION

Taken together, our findings show for the first time that the 695 amino acid isoform of APP is capable of promoting EMT in a prostate cancer cell line. The mechanism of action is likely to involve signalling via the cytosolic domain of the protein and also the E1 copper binding region within the extracellular domain of the protein. However, it is clear that, whilst these factors are prerequisites for APP-induced EMT, there must be additional properties specific to APP_{695} that participate in the phenomenon given the fact that the larger APP_{751} and APP_{770} isoforms do not act in a similar manner. Thus, the repression of APP_{695} expression may represent a therapeutic strategy for reducing the metastatic potential of prostate cancer cells.

COMPETING INTERESTS

The authors have declared that no competing interests exist.

REFERENCES

1. Prins GS, Putz O. Molecular signaling pathways that regulate prostate gland development. Differentiation. 2008;76(6): 641-59.
2. Marker PC, Donjacour AA, Dahiya R, Cunha GR. Hormonal, cellular, and

molecular control of prostatic development. Dev Biol. 2003;253(2):165-74.

3. Hayward SW, Cunha GR. The prostate: development and physiology. Radiol Clin North Am. 2000;38(1):1-14.

4. Kalluri R, Weinberg RA. The basics of epithelial-mesenchymal transition. J Clin Invest. 2009;119(6):1420-8.

5. Gough M, Parr-Sturgess C, Parkin E. Zinc metalloproteinases and amyloid Beta-Peptide metabolism: the positive side of proteolysis in Alzheimer's disease. Biochem Res Int. 2011;2011:721463.

6. Meng JY, Kataoka H, Itoh H, Koono M. Amyloid beta protein precursor is involved in the growth of human colon carcinoma cell in vitro and in vivo. Int J Cancer. 2001;92(1):31-9.

7. Ko SY, Lin SC, Chang KW, Wong YK, Liu CJ, Chi CW, et al. Increased expression of amyloid precursor protein in oral squamous cell carcinoma. Int J Cancer. 2004;111(5):727-32.

8. Krause K, Karger S, Sheu SY, Aigner T, Kursawe R, Gimm O, et al. Evidence for a role of the amyloid precursor protein in thyroid carcinogenesis. J Endocrinol. 2008;198(2):291-9.

9. Hansel DE, Rahman A, Wehner S, Herzog V, Yeo CJ, Maitra A. Increased expression and processing of the Alzheimer amyloid precursor protein in pancreatic cancer may influence cellular proliferation. Cancer Res 2003;63(21):7032-7.

10. Takayama K, Tsutsumi S, Suzuki T, Horie-Inoue K, Ikeda K, Kaneshiro K, et al. Amyloid precursor protein is a primary androgen target gene that promotes prostate cancer growth. Cancer Res 2009;69(1):137-42.

11. Miyazaki T, Ikeda K, Horie-Inoue K, Inoue S. Amyloid precursor protein regulates migration and metalloproteinase gene expression in prostate cancer cells.

Biochem Biophys Res Commun. 2014;452(3):828-833.

12. Latasa MJ, Belandia B, Pascual A. Thyroid hormones regulate beta-amyloid gene splicing and protein secretion in neuroblastoma cells. Endocrinology. 1998;139(6):2692-8.

13. Smith PK, Krohn RI, Hermanson GT, Mallia AK, Gartner FH, Provenzano MD, et al. Measurement of protein using bicinchoninic acid. Anal Biochem. 1985;150(1):76-85.

14. Hooper NM, Turner AJ. Isolation of two differentially glycosylated forms of peptidyl-dipeptidase A (angiotensin converting enzyme) from pig brain: a re-evaluation of their role in neuropeptide metabolism. Biochem J. 1987;241(3):625-33.

15. von Rotz RC, Kohli BM, Bosset J, Meier M, Suzuki T, Nitsch RM, et al. The APP intracellular domain forms nuclear multiprotein complexes and regulates the transcription of its own precursor. J Cell Sci. 2004;117(Pt 19):4435-48.

16. Belyaev ND, Kellett KA, Beckett C, Makova NZ, Revett TJ, Nalivaeva NN, et al. The transcriptionally active amyloid precursor protein (APP) intracellular domain is preferentially produced from the 695 isoform of APP in a {beta}-secretase-dependent pathway. J Biol Chem. 2010;285(53):41443-54.

17. Gough M, Blanthorn-Hazell S, Delury C, Parkin E. The E1 copper binding domain of full-length amyloid precursor protein mitigates copper-induced growth inhibition in brain metastatic prostate cancer DU145 cells. Biochem Biophys Res Commun; 2014.

18. Kong GK, Miles LA, Crespi GA, Morton CJ, Ng HL, Barnham KJ, et al. Copper binding to the Alzheimer's disease amyloid precursor protein. Eur Biophys J; 2007.